Inhibition of Endoplasmic Reticulum Stress Reverses Synaptic Plasticity Deficits in Striatum of DYT1 Dystonia Mice

Huaying Cai
Zhejiang University School of Medicine Sir Run Run Shaw Hospital https://orcid.org/0000-0002-8333-9194

Linhui Ni
Zhejiang University School of Medicine Sir Run Run Shaw Hospital

Xingyue Hu
Shao Yifu Hospital: Zhejiang University School of Medicine Sir Run Run Shaw Hospital

Xianjun Ding (xkxjz2009@126.com)
Zhejiang University School of Medicine Sir Run Run Shaw Hospital

Research Article

Keywords: DYT1 dystonia, endoplasmic reticulum stress, striatal synaptic plasticity, TUDAC

Posted Date: February 8th, 2021

DOI: https://doi.org/10.21203/rs.3.rs-166434/v1

Abstract

Background & objective

Striatal plasticity alterations caused by endoplasmic reticulum (ER) stress is supposed to be critically involved in the mechanism of DYT1 dystonia. In the current study, we expanded this research field by investigating the critical role of ER stress underlying synaptic plasticity impairment imposed by mutant heterozygous Tor1a$^{+/-}$ in a DYT1 dystonia mouse model.

Methods & results

Long-term depression (LTD) was failed to be induced, while long-term potentiation (LTP) was further strengthened in striatal spiny neurons (SPNs) from the Tor1a$^{+/-}$ DYT1 dystonia mice. Spine morphology analyses revealed a significant increase of both number of mushroom type spines and spine width in Tor1a$^{+/-}$ SPNs. In addition, increased AMPA receptor function and the reduction of NMDA/AMPA ratio in the postsynaptic of Tor1a$^{+/-}$ SPNs was observed, along with increased ER stress protein levels in Tor1a$^{+/-}$ striatum. Notably, ER stress inhibitors, tauroursodeoxycholic acid (TUDCA), could rescue LTD as well as AMPA currents.

Conclusion

The current study illustrated the role of ER stress in mediating structural and functional plasticity alterations in Tor1a$^{+/-}$ SPNs. Inhibition of the ER stress by TUDCA is beneficial in reversing the deficits at the cellular and molecular levels. Remedy of dystonia associated neurological and motor functional impairment by ER stress inhibitors could be a recommendable therapeutic agent in clinical practice.

Introduction

DYT1 dystonia is a complex neurological condition characterized by abnormal involuntary movements or postures [1], usually caused by a GAG base-pair deletion in the DYT1 gene coding for Tor1a protein [2]. Although it has been recognized that the onset of movement disorder in DYT1 dystonia is between childhood and adolescence, what triggers the manifestation of clinical symptoms is still unknown [3]. Human studies have indicated synaptic plasticity alterations as major determinants in dystonia pathophysiology [4]. Plasticity impairments, including functional and structural synaptic deficits, could lead to motor learning disabilities [5]. Furthermore, patterns of impaired motor learning have also been described in clinically unaffected DYT1 mutation carriers, which further supports the notion that aberrant plasticity might be a unique endophenotype of dystonia [6]. Of note, an impairment of striatal plasticity has been explored in a number of different dystonia rodent models, including knock-in mice heterozygous for Tor1a [7,8], which presented a remarkable similarity to the studies in dystonia patients [9]. Hence, the current evidence supports the judgement that DYT1 dystonia is a complex neurodevelopmental disorder with impaired striatal plasticity and motor dysfunction.

Although impairments in structural and functional synaptic plasticity have been suggested based on rodent models [10], which could help explain clinical demonstrations in dystonia patients, the specific mechanisms underlying the chain of events from synaptic plasticity to dystonia are still elusive. To date, several potential mechanisms have been put forward to be relevant, including increased reactive oxygen species (ROS) production [11], neuroinflammation [12], and reduced brain-derived neurotrophic factor (BDNF) production [13]. As a malignant consequence of ROS, the role of endoplasmic reticulum (ER) stress response, which may lead to critical cellular malfunction and even neuronal apoptosis [14], has been underestimated. In recent years, researches have suggested that ER stress contributes to a variety of neurodegenerative diseases [15,16]. Activating transcription factor-4 (ATF-4) and C/EBP homologous protein (CHOP), two marker proteins of ER stress, were also upregulated under condition of neurodegenerative disease-related cell death [17]. Hence, we speculate that ER stress may play a crucial role in underlying deficits in neuroplasticity and motor function in dystonia.

Whereas, to date, the relationship between ER stress and corticostriatal plasticity in dystonia is still lacking. Moreover, whether functional and structural plasticity abnormalities could be reversed by inhibition of ER stress remains unknown. Here, we confirmed structural and functional abnormalities of striatal synapse plasticity exhibiting in Tor1a$^{+/-}$ mice, which is paralleled by a significant increase in ER stress markers protein levels, along with the increased AMPA receptor function and the reduction of NMDA/AMPA ratio in the postsynaptic of Tor1a$^{+/-}$ spiny projection neurons (SPNs). Notably, ER stress inhibitors, TUDCA, could rescue LTD as well as AMPA currents. Our results illustrate potential molecular, functional and structural changes in Tor1a$^{+/-}$ SPNs, demonstrating the link between abnormal plasticity and ER stress in dystonia. Revelation the mechanism by which synaptic plasticity are altered could point out new routes for the treatment and prevention of dystonia.

Materials And Methods

Heterozygous Tor1a$^{+/-}$ mouse model for DYT1 dystonia

Animal experiments were performed in accordance with the guidelines for the use of animals in biomedical research [18]. The experimental procedures were approved by the Internal Institutional Review Committee of Zhejiang University (ZJU-2020-01-06). All efforts were made to minimize the number of animals and their suffering. Male heterozygous Tor1a$^{+/-}$ and their wild-type littermates (Tor1a$^{+/+}$; Jackson Laboratory, Bar Harbor, ME, USA), were used. The preparation of corticostriatal slices and genotyping was performed as previously described [19]. Wild-type and mutant mice from post-natal day P25 to P35 were randomly distributed to experimental and control groups. Researchers conducting experiments and data analyses were blind to genotype and treatment.

Brain slice preparation

Mice were sacrificed by cervical dislocation, brains removed and sliced with a vibratome (Leica Microsystems) in oxygenated Krebs' solution (in mM: 126 NaCl, 2.5 KCl, 1.3 $MgCl_2$, 1.2 NaH_2PO_4, 2.4

$CaCl_2$, 10 glucose, 18 $NaHCO_3$). Coronal and parasagittal corticostriatal slices (200-300 mm) were incubated in Krebs' solution at room temperature for 30 min. Then, individual slices were transferred into recording chambers continuously superfused with Krebs' solution (32-33˚C) saturated with 95% O_2 and 5% CO_2.

Patch-clamp recordings

Patch-clamp recordings was performed as previously described [20]. For voltage-clamp experiments, pipettes (2.5-5 MΩ) were filled with Cs^+ internal solution (in mM: 120 $CsMeSO_3$, 15 CsCl, 8 NaCl, 10 TEA-Cl, 10 HEPES, 0.2 EGTA, 2 Mg-ATP, and 0.3 Na-GTP; pH 7.3 adjusted with CsOH; 300 mOsm). For whole-cell recordings of glutamatergic sEPSCs, SPNs were clamped at HP=-70 mV in the presence of the GABAA receptor antagonist PTX (50 mM). For GABAergic sIPSCs, SPNs were recorded at HP=+10 mV in MK801 (30 mM) and CNQX (10 mM) to block NMDARs and AMPARs, respectively. Both mEPSCs and mIPSCs were recorded by adding 1 mM TTX. PPR was measured at HP=-70 mV in PTX by delivering two stimuli at 25-1000 ms ISI. Synaptic strength was measured by the NMDAR/AMPAR ratio at HP=+40 mV in PTX. The AMPAR-mediated component of EPSC was isolated in MK-801 and the NMDAR component was obtained by digital subtraction of the AMPAR component from the dual-component EPSC. The AMPAR and NMDAR IV relationships were measured in the presence of PTX plus MK-801 or CNQX, respectively. The RI was calculated as ratio of the mean EPSC amplitudes measured at +40 mV and -70 mV.

Current-clamp recordings

Current-clamp recordings of SPNs were conducted with intracellular electrodes filled as previously described [21]. Corticostriatal EPSPs were recorded in PTX (50 mM). HFS (three trains 100 Hz, 3 s, 20 s apart) was delivered at suprathreshold intensity to induce LTD. Magnesium was omitted to optimize LTP induction. Average EPSP amplitude was plotted over-time as percentage of control pre-HFS amplitude.

Western blotting, quantitative real-time PCR and RNA-Seq analysis

To quantify postsynaptic signaling proteins in striatum, subcellular fractionation of striatal tissue was prepared for western blotting, quantitative real-time PCR and RNA-Seq analysis as previously described [22]. Detailed information was presented in Supplemental Materials.

Immunohistochemistry

Striatal changes of the direct and indirect pathways were investigated via immunofluorescence (IF) as previously described [23]. In brief, 20~30 μm thick sections were cut from each slice with a freezing microtome, then dehydrated with serial alcohol dilutions. We applied the following primary antibodies: rabbit monoclonal anti-DARPP32 (1:100, ab40801, Abcam), rabbit polyclonal anti-Enkephalin (5 μg/ml, ab85798, Abcam). Images were obtained with a confocal laser scanning microscope (LSM700 Zeiss) and analyzed via ImageJ.

Spine morphology

Golgi-Cox staining was conducted to observe spine morphology of SPNs, as previously described [24]. Briefly, brain tissues were stained via the Rapid Golgi Staining Kit (FD Neuro-Technologies). Then, SPNs from the striatum were observed under Zeiss Microscope. Apical dendrites with spines from 10 neurons for each slice were traced through a 60× lens to measure spine density. Next, the number of spines per 10 μm length was calculated. Furthermore, spine subtypes were defined via the relative proportion of the length, head diameter, and neck diameter of spine.

Drug treatment

Tauroursodeoxycholic acid (TUDCA, Sigma-Aldrich) was dissolved in phosphate-buffered saline (PBS) of pH 7.4 at a concentration of 7.8 mg/ml according to the manufacturer protocol. As previously described [25], TUDCA was daily intraperitoneally injected (100 mg/kg) for 14 days. The mice were randomly assigned into four groups: the PBS-treated Tor1a$^{+/+}$ mice, TUDCA-treated Tor1a$^{+/+}$ mice, PBS-treated Tor1a$^{+/-}$ mice, and TUDCA-treated Tor1a$^{+/-}$ mice. Data for PBS-treated mice was not shown in the results.

Statistical analysis

Data were analyzed with ClampFit (Molecular Devices) and GraphPad Prism (GraphPad) software. All data were obtained from at least three independent experiments and are represented as mean ± SEM. Statistical significance was evaluated using Student's t test, one-way ANOVA or two-way ANOVA with post-hoc test for group comparisons. Statistical tests were two-tailed, the confidence interval (CI) was 95%, and the statistical significance was set at $P<0.05$.

Results

Altered striatal long-term synaptic plasticity in Tor1a$^{+/-}$ mice

We firstly explored intrinsic and synaptic properties of SPNs from juvenile (P25-P35) mice. SPNs recorded from both Tor1a$^{+/+}$ and Tor1a$^{+/-}$ mice did not exhibit significant differences in their intrinsic membrane properties (Supplementary Figure S1). Then, we explored the characteristics of LTD and LTP from Tor1a$^{+/+}$ and Tor1a$^{+/-}$ mice. In Tor1a$^{+/-}$ SPNs, the HFS stimulation failed to cause a synaptic depression (Figure 1A; $P>0.05$), while a robust LTD was elicited in Tor1a$^{+/+}$ SPNs ($P<0.05$). Furthermore, the LTP induction protocol induced a stable LTP in Tor1a$^{+/+}$ SPNs (Figure 1B; $P<0.05$). Not surprisingly, in Tor1a$^{+/-}$ SPNs LTP showed a tendency to increase compared with wild-type SPNs, indicating a hyperexcitability (Tor1a$^{+/+}$: 148.80 ± 15.39% of pre-HFS; Tor1a$^{+/-}$: 172.35 ± 11.06% of pre-HFS; $P<0.05$).

At excitatory synapses, NMDARs form a unique cluster mainly at the center of the PSD, while AMPARs segregate in clusters surrounding the NMDARs, and the balance of them affects the synaptic transmission properties of a unitary synapse [26]. Hence, NMDAR/AMPAR current ratios at corticostriatal synapses were recorded, in order to unmask the electrophysiological physiology of AMPARs and

NMDARs currents in SPNs from both Tor1a$^{+/+}$ and Tor1a$^{+/-}$ mice. The results revealed that the NMDAR/AMPAR ratio significantly decreased in Tor1a$^{+/-}$ SPNs compared to Tor1a$^{+/+}$ SPNs (Figure 1C; P<0.05), indicating an enhanced AMPARs abundance relative to NMDARs quantity.

3.2 Altered molecular markers and morphology of synapse in Tor1a$^{+/-}$ mice

To identify potential mechanism of direct- and indirect-pathway SPNs, confocal images were obtained from two SPNs recorded in Tor1a$^{+/-}$ and Tor1a$^{+/+}$ slices. Recording electrodes were filled with biocytin (pink) and SPNs were immunolabelled with anti-ENK (green) and anti-DARPP-32 (red). Immunofluorescence staining indicated that ENK-negative SPNs from Tor1a$^{+/-}$ failed to induce LTD (upper panel of Figure 2A), while SPNs from Tor1a$^{+/+}$ slices exhibited to be ENK-positive (lower panel of Figure 2A), indicating a possible inhibition of indirect-pathway in SPNs from Tor1a$^{+/-}$ slices.

Moreover, the levels of AMPAR and NMDAR subunits were evaluated using WB analysis. A significant increase in the levels of AMPAR subunits (p-GluA1-Ser845 and GluA2, but not GluA1) in the striatal tissues of Tor1a$^{+/-}$ mice compared to wild-types (Figure 2B&C; both P<0.05), which consistent with the above-described electrophysiological results of a reduction of the NMDA/AMPA ratio. Interestingly, we also observed an increase of NMDAR2A but not NMDAR2B subunit in the postsynaptic compartment of Tor1a$^{+/-}$ mice (P<0.05). However, we didn't observe a significant alteration in PSD-95 (P>0.05), which is known to be involved in maturation of excitatory synapses [27].

In addition, we further evaluated spine morphology in Tor1a$^{+/-}$ SPNs, compared to Tor1a$^{+/+}$ SPNs. Tor1a$^{+/-}$ SPNs exhibited an overall decrease of dendritic spine density (Figure 2D&E). In addition, a larger number of mushroom-type spines (Figure 2G; P<0.05) and a concomitant a smaller number of stubby-type spines were found compared to Tor1a$^{+/+}$ SPNs (Figure 2G; P<0.05), though no significant difference was found for dendritic spine length and head width (Figure 2F; P>0.05). Consequently, these alterations were associated, to an advanced stage of spine maturation.

3.3 Abnormal eIF2α signaling and ER stress in Tor1a$^{+/-}$ mice

Impairment of eIF2α signaling, which is known for its roles in cellular stress responses and synaptic plasticity, was identified in patients with idiopathic dystonia [8]. Hence, we speculated that mutant Tor1a in DYT1 mice might lead to basal abnormalities in the eIF2a signaling and ER stress. We tried to validate this hypothesis in heterozygous Tor1a$^{+/-}$ mouse model for DYT1 dystonia. After RNA-Seq analysis of striatal tissue was performed, the DEGs were then analyzed using Ingenuity Pathway Analysis (IPA) to identify dysregulated canonical pathways (Figure 3A). As expected, eIF2a signaling was one of the top up-regulated pathways in Tor1a$^{+/-}$ mouse, which was further confirmed by GSEA analysis (Figure 3B). Notably, synaptic plasticity associated pathways were also dysregulated, with LTD down-regulated and LTP up-regulated.

Tor1a expression has been suggested to alter the cellular response to acute ER stress [28]. Whereas, it has not been validated in striatum of DYT1 knock-in mice. RT-qPCR showed a significant increase in striatal transcript levels for Chop, Bip, and Atf4 (all $P<0.05$), but not for eIF2α ($P>0.05$), in Tor1a$^{+/-}$ mice compared with the wild-type controls (Figure 3C), indicating induction of ER stress. Similarly, WB for expression of the components of eIF2α signaling further confirmed the activation of eIF2α signaling and induction of ER stress (Figure 3D&E).

3.4 ER stress inhibitor rescues long-term memory deficit in Tor1a$^{+/-}$ mice

To investigate whether activation of ER stress was involved in the long-term synaptic plasticity deficits in Tor1a$^{+/-}$ mice, eIF2α signaling was selectively blocked by the TUDAC. Firstly, we investigated the effect of TUDCA on the expression of ER stress markers. As expected, the results of RT-qPCR and WB consistently revealed that the levels of these proteins (p-eIF2α, Chop, Bip, and Atf4) in striatal tissues of Tor1a$^{+/-}$ mice were significantly reduced after treatment with TUDCA (Supplementary Figure S1). Then, the influence of ER stress on the abnormal regulation of AMPA currents and in the synaptic plasticity deficits was observed. After repetitive treatment with TUDAC (100 mg/kg, intraperitoneally), corticostriatal LTD was completely rescued in Tor1a$^{+/-}$ mice (Figure 4A; $P<0.05$). In addition, TUDAC treatment reduced LTP amplitude in Tor1a$^{+/-}$ mice (Figure 4B; $P>0.05$). Similarly, treatment with TUDAC completely normalized the NMDAR/AMPAR ratio in Tor1a$^{+/-}$ mice (Figure 4C; $P>0.05$). The IV curve of AMPAR-EPSC also revealed no significant difference between genotypes (Figure 4D; $P>0.05$). In PBS-treated Tor1a$^{+/+}$ and Tor1a$^{+/-}$ mice, no significant change was found (data not shown).

Furthermore, we also evaluated spine morphology in Tor1a$^{+/+}$ and Tor1a$^{+/-}$ SPNs after treatment with TUDAC (Figure 4E). Tor1a$^{+/-}$ SPNs returned to a normalization of spine density (Figure 4G; $P>0.05$) and of spine size (Figure 4F; $P>0.05$) compared to Tor1a$^{+/+}$ SPNs. Interestingly, the number of mushrooms in Tor1a$^{+/-}$ SPNs sharply decreased to a lower level than that of Tor1a$^{+/+}$ SPNs, along with a significant increase of thin spines (Figure 4H; $P<0.05$), which could be due to an over-reaction to TUDAC in Tor1a$^{+/-}$ SPNs. Further evidence of TUDAC could reverse alteration molecular markers for synapse plasticity was presented in Supplementary Figure S3, which was also consistent with the above results. These data suggest that activated ER stress is a potential cause of the abnormal developmental expression of AMPARs on SPN postsynaptic membranes, further resulting in synaptic plasticity deficits in Tor1a$^{+/-}$ mice.

Discussion

Although the role of activated ER stress in DYT1 dystonia has been previously explored in vitro and in vivo [29-31], these studies revealed to be limited for the study of ER stress via DYT1 dystonia mouse model. In the current study, we expanded this research field by investigating the critical role of ER stress underlying synaptic plasticity impairment imposed by mutant heterozygous Tor1a$^{+/-}$ in a DYT1 dystonia mouse model. We obtained evidence from different aspects to support this conclusion. First, Tor1a$^{+/-}$

mice revealed activated ER stress in the striatum accompanied by upregulation of p-eIF2α, Chop, Bip, and Atf4, sensitive indicators of ER stress [32,33]. The ER stress inhibitor, TUDCA, could specifically reverse these effects in Tor1a$^{+/-}$ mice. Second, structural changes in the synapses in the striatal subfield in Tor1a$^{+/-}$ mice were also repaired by inhibition of ER stress. Third, at the electrophysiology level, suppression of ER stress by TUDCA could completely rescue the impairment in LTD in Tor1a$^{+/-}$ mice. Taken together, the above results indicated that synaptic plasticity impairment in Tor1a$^{+/-}$ mice could be partially due to the activation of ER stress in the striatum, which further results in deficits of structural and functional synaptic plasticity. Inhibition of activated ER stress might correct these alterations and is therefore beneficial for motor function recovery in DYT dystonia.

Recent researches have proposed a correlation between eIF2α signaling and dystonia in DYT1 rodent model and dystonia patients [34,8]. In this study, we conducted a comprehensive transcriptomic analysis in the striatal tissues from DYT1 dystonia mice brain, which provided another piece of bioinformatic evidence supporting this association. Whereas, it remains unknown whether dysregulation of eIF2α signaling plays a pathogenic role in DYT1 dystonia, or it is unrelated to DYT1 dystonia simply as a byproduct of Tor1a$^{+/-}$ mutant. Intriguingly, the electrophysiological deficits and synapse morphology alterations observed in Tor1a$^{+/-}$ mice, are partially or completely rescued after inhibition of the eIF2a signaling by TUDCA, indicating a potential pathogenic relevance. In addition, RT-PCR and WB analyses also found transcriptional dysregulation of eIF2α signaling in striatum tissues from Tor1a$^{+/-}$ mice. Hence, all these findings confirmed a relationship between DYT1 dystonia and eIF2α dysregulation, which might further lead to an abnormal response to ER stress in Tor1a$^{+/-}$ mice. On the one hand, the role of eIF2α signaling has been dependent on homeostatic physiological systems to regulate neurobiological processes, including synaptic plasticity and neurite maturation [35,36]. Since DYT1 dystonia is a type of neurodevelopmental disorders, Tor1a$^{+/-}$ mutation might trigger the pathogenic process through ER stress-dependent way. On the other hand, eIF2α dysregulation may play a compensatory role in response to DYT1-mediated biological processes [37]. However, all these suspects are critical questions waiting to be addressed in the future, as they harbor significant potential in illuminating the mechanism of DYT1 dystonia pathology.

Although one of the most remarkable detrimental results of ER stress in striatum is neuronal apoptosis, which contributes to the neurological impairments [38], we also observed subtle alterations in the synapse morphology, namely reduction in the density of spines and increase in the number of mushroom-type spines. These results are consistent with previous studies suggesting that activation of ER stress could lead to synaptic degeneration and interrupt neurotransmission related to changes in synaptic morphology [39]. The finding that the density of spines is significantly reduced in Tor1a$^{+/-}$ SPNs further supports the idea that subtle functional and structural alterations in SPNs contribute to neurological malfunctions in dystonia. Notably, our finding of no significant alteration in PSD-95 expression, a critical protein in synapse maturation and reconstruction of mushroom-type spines [40], could be controversial. This may be associated with chaotic unfolded proteins reactions corresponding to ER stress. Besides, ubiquitin-proteasome system activated by ER stress could induce protein degradation and might play a

role in maintaining the homeostasis and localization of several postsynaptic proteins, such as PSD-95 [41].

As described in the current study, along with molecular and structural changes at striatal synapses, electrophysiological alterations also revealed in SPNs from Tor1a$^{+/-}$ mice. Striatal LTP is suspected to be dependent on the activation of NMDAR, while LTD depends on AMPAR [42,43]. The electrophysiological and WB analyses indicated a significant increase in AMPAR-mediated currents, along with the decreased NMDAR/AMPAR ratio in SPNs from Tor1a$^{+/-}$ mice. A potential regulatory mechanism for synaptic plasticity relies on the balance between synaptic insertion into the postsynaptic membrane and glutamate receptors removal from the counterparts [44]. In brief, increased AMPA receptor function and abundance in into the postsynaptic membrane could lead to the dyshomeostasis of excitatory synapses. As our results presented, both GluA1 and GluA2 subunits of AMPARs in the post-synaptic membrane of Tor1a$^{+/-}$ SPNs significantly increased, indicating an increased AMPA receptor abundance. Notably, the phosphorylation of GluA1-Ser845 (p-GluA1) is over-expressed in Tor1a$^{+/-}$ mice, which is consistent with a well-established relationship between p-GluA1 and LTP [42]. In detail, p-GluA1 mainly takes part in the synaptic delivery of GluA1-containing AMPARs via LTP and might play an indispensable role in post-synaptic membrane stabilization for AMPARs. Hence, we have reasons to believe that the aberrant composition of striatal AMPARs may be involved in the loss of LTD in Tor1a$^{+/-}$ mice.

Alterations of spine morphology are supposed to be dependent on the composition of NMDARs and AMPARs and synaptic plasticity function, which further determine the long-term structural plasticity [45]. In Tor1a$^{+/-}$ mice, an increase in the number of mushroom spines was found to be accompanied by a decrease in spine density, which is a sign of ‘hyperexcitability’. It has been acknowledged that expression patterns of the NMDAR2 subunits of NMDARs at dendritic spines become prevalently existed and abundant throughout the striatum after more than two postnatal weeks [46,47]. In addition, a previous research has proposed that there is a positive correlation between spine size and the strength of AMPAR-mediated current at synaptic post-membranes [48]. In consistent with these findings, in Tor1a$^{+/-}$ mice, we also found a significant increase of both GluA1 and GluA2 subunits of AMPARs accompanied by a concomitant increase of spine head width and the number of mushroom spines.

The current study firstly conducted a comprehensive investigation on whether ER stress plays a critical role in underlying impairment in neuroplasticity base on a DYT1 dystonia mouse model. The results demonstrated that the activation of ER stress was induced by upregulation of Atf-4 and Chop. In addition, spine morphology of striatal synapses was change probably due to ER stress-induced protein degradation, which resulted in the impairment of synaptic plasticity. Both effects contribute to the loss of LTD and motor deficits. Notably, TUDAC, an inhibitor of ER stress, could rescued LTD and AMPAR currents alteration. Our study illuminates that inhibition of ER stress could be a potential treatment strategy for neuronal protection in dystonia.

In conclusion, the current study suggests that the activation of ER stress might play a key role in synapse plasticity deficits in Tor1a$^{+/-}$ striatum SPNs. Accumulation of misfolded proteins (eIF2α, Chop, Bip, and

Atf4) and altered levels of AMPAR and NMDAR subunits could result in disordered neurological functions and impaired synaptic plasticity in striatum that underlie motor function and coordination. Inhibition of the ER stress by TUDCA is beneficial in reversing the deficits at the cellular and molecular levels. Considering the everlasting efforts in pharmaceutical industries and researchers to find out more therapeutic treatments in ameliorating dystonia, remedy of dystonia associated neurological and motor functional impairment by ER stress inhibitors could be a recommendable therapeutic agent in clinical practice.

Declarations

Funding

This study was supported by the Natural Science Foundation of China (No.81400926 for Huaying Cai), the Natural Science Foundation of Zhejiang Province of China (LY19H090027 for Huaying Cai), and the Medical and Health Research Project of Zhejiang Province of China (2018RC045 for Huaying Cai), the Natural Science Foundation of Zhejiang Province of China (LY16H060002 for Xianjun Ding).

Conflict of interest

The authors declare that they have no conflict of interest.

References

1. Goodchild RE, Grundmann K, Pisani A (2013) New genetic insights highlight 'old' ideas on motor dysfunction in dystonia. Trends Neurosci 36 (12):717-725. doi:10.1016/j.tins.2013.09.003
2. Ledoux MS, Dauer WT, Warner TT (2013) Emerging common molecular pathways for primary dystonia. Mov Disord 28 (7):968-981. doi:10.1002/mds.25547
3. Jahanshahi M, Torkamani M (2017) The cognitive features of idiopathic and DYT1 dystonia. Mov Disord 32 (10):1348-1355. doi:10.1002/mds.27048
4. Quartarone A, Hallett M (2013) Emerging concepts in the physiological basis of dystonia. Mov Disord 28 (7):958-967. doi:10.1002/mds.25532
5. Arkadir D, Radulescu A, Raymond D, Lubarr N, Bressman SB, Mazzoni P, Niv Y (2016) DYT1 dystonia increases risk taking in humans. Elife 5. doi:10.7554/eLife.14155
6. Quartarone A, Rizzo V, Terranova C, Morgante F, Schneider S, Ibrahim N, Girlanda P, Bhatia KP, Rothwell JC (2009) Abnormal sensorimotor plasticity in organic but not in psychogenic dystonia. Brain 132 (Pt 10):2871-2877. doi:10.1093/brain/awp213
7. Martella G, Maltese M, Nistico R, Schirinzi T, Madeo G, Sciamanna G, Ponterio G, Tassone A, Mandolesi G, Vanni V, Pignatelli M, Bonsi P, Pisani A (2014) Regional specificity of synaptic plasticity deficits in a knock-in mouse model of DYT1 dystonia. Neurobiol Dis 65:124-132. doi:10.1016/j.nbd.2014.01.016

8. Rittiner JE, Caffall ZF, Hernandez-Martinez R, Sanderson SM, Pearson JL, Tsukayama KK, Liu AY, Xiao C, Tracy S, Shipman MK, Hickey P, Johnson J, Scott B, Stacy M, Saunders-Pullman R, Bressman S, Simonyan K, Sharma N, Ozelius LJ, Cirulli ET, Calakos N (2016) Functional Genomic Analyses of Mendelian and Sporadic Disease Identify Impaired eIF2alpha Signaling as a Generalizable Mechanism for Dystonia. Neuron 92 (6):1238-1251. doi:10.1016/j.neuron.2016.11.012
9. Balint B, Mencacci NE, Valente EM, Pisani A, Rothwell J, Jankovic J, Vidailhet M, Bhatia KP (2018) Dystonia. Nat Rev Dis Primers 4 (1):25. doi:10.1038/s41572-018-0023-6
10. Peterson DA, Sejnowski TJ, Poizner H (2010) Convergent evidence for abnormal striatal synaptic plasticity in dystonia. Neurobiol Dis 37 (3):558-573. doi:10.1016/j.nbd.2009.12.003
11. Luthy K, Mei D, Fischer B, De Fusco M, Swerts J, Paesmans J, Parrini E, Lubarr N, Meijer IA, Mackenzie KM, Lee WT, Cittaro D, Aridon P, Schoovaerts N, Versees W, Verstreken P, Casari G, Guerrini R (2019) TBC1D24-TLDc-related epilepsy exercise-induced dystonia: rescue by antioxidants in a disease model. Brain 142 (8):2319-2335. doi:10.1093/brain/awz175
12. Hinarejos I, Machuca-Arellano C, Sancho P, Espinos C (2020) Mitochondrial Dysfunction, Oxidative Stress and Neuroinflammation in Neurodegeneration with Brain Iron Accumulation (NBIA). Antioxidants (Basel) 9 (10). doi:10.3390/antiox9101020
13. Martino D, Muglia M, Abbruzzese G, Berardelli A, Girlanda P, Liguori M, Livrea P, Quattrone A, Roselli F, Sprovieri T, Valente EM, Defazio G (2009) Brain-derived neurotrophic factor and risk for primary adult-onset cranial-cervical dystonia. Eur J Neurol 16 (8):949-952. doi:10.1111/j.1468-1331.2009.02633.x
14. Prentice H, Modi JP, Wu JY (2015) Mechanisms of Neuronal Protection against Excitotoxicity, Endoplasmic Reticulum Stress, and Mitochondrial Dysfunction in Stroke and Neurodegenerative Diseases. Oxid Med Cell Longev 2015:964518. doi:10.1155/2015/964518
15. Martinez G, Khatiwada S, Costa-Mattioli M, Hetz C (2018) ER Proteostasis Control of Neuronal Physiology and Synaptic Function. Trends Neurosci 41 (9):610-624. doi:10.1016/j.tins.2018.05.009
16. Roussel BD, Kruppa AJ, Miranda E, Crowther DC, Lomas DA, Marciniak SJ (2013) Endoplasmic reticulum dysfunction in neurological disease. Lancet Neurol 12 (1):105-118. doi:10.1016/S1474-4422(12)70238-7
17. Kasetti RB, Patel PD, Maddineni P, Patil S, Kiehlbauch C, Millar JC, Searby CC, Raghunathan V, Sheffield VC, Zode GS (2020) ATF4 leads to glaucoma by promoting protein synthesis and ER client protein load. Nat Commun 11 (1):5594. doi:10.1038/s41467-020-19352-1
18. Percie du Sert N, Hurst V, Ahluwalia A, Alam S, Avey MT, Baker M, Browne WJ, Clark A, Cuthill IC, Dirnagl U, Emerson M, Garner P, Holgate ST, Howells DW, Karp NA, Lazic SE, Lidster K, MacCallum CJ, Macleod M, Pearl EJ, Petersen OH, Rawle F, Reynolds P, Rooney K, Sena ES, Silberberg SD, Steckler T, Wurbel H (2020) The ARRIVE guidelines 2.0: Updated guidelines for reporting animal research. Br J Pharmacol 177 (16):3617-3624. doi:10.1111/bph.15193
19. Goodchild RE, Kim CE, Dauer WT (2005) Loss of the dystonia-associated protein torsinA selectively disrupts the neuronal nuclear envelope. Neuron 48 (6):923-932. doi:10.1016/j.neuron.2005.11.010

20. Sciamanna G, Tassone A, Martella G, Mandolesi G, Puglisi F, Cuomo D, Madeo G, Ponterio G, Standaert DG, Bonsi P, Pisani A (2011) Developmental profile of the aberrant dopamine D2 receptor response in striatal cholinergic interneurons in DYT1 dystonia. PLoS One 6 (9):e24261. doi:10.1371/journal.pone.0024261
21. Cummins TR, Rush AM, Estacion M, Dib-Hajj SD, Waxman SG (2009) Voltage-clamp and current-clamp recordings from mammalian DRG neurons. Nat Protoc 4 (8):1103-1112. doi:10.1038/nprot.2009.91
22. Baucum AJ, 2nd, Brown AM, Colbran RJ (2013) Differential association of postsynaptic signaling protein complexes in striatum and hippocampus. J Neurochem 124 (4):490-501. doi:10.1111/jnc.12101
23. Capper-Loup C, Kaelin-Lang A (2013) Locomotor velocity and striatal adaptive gene expression changes of the direct and indirect pathways in Parkinsonian rats. J Parkinsons Dis 3 (3):341-349. doi:10.3233/JPD-130202
24. Xu LH, Xie H, Shi ZH, Du LD, Wing YK, Li AM, Ke Y, Yung WH (2015) Critical Role of Endoplasmic Reticulum Stress in Chronic Intermittent Hypoxia-Induced Deficits in Synaptic Plasticity and Long-Term Memory. Antioxid Redox Signal 23 (9):695-710. doi:10.1089/ars.2014.6122
25. Castro-Caldas M, Carvalho AN, Rodrigues E, Henderson CJ, Wolf CR, Rodrigues CM, Gama MJ (2012) Tauroursodeoxycholic acid prevents MPTP-induced dopaminergic cell death in a mouse model of Parkinson's disease. Mol Neurobiol 46 (2):475-486. doi:10.1007/s12035-012-8295-4
26. Goncalves J, Bartol TM, Camus C, Levet F, Menegolla AP, Sejnowski TJ, Sibarita JB, Vivaudou M, Choquet D, Hosy E (2020) Nanoscale co-organization and coactivation of AMPAR, NMDAR, and mGluR at excitatory synapses. Proc Natl Acad Sci U S A 117 (25):14503-14511. doi:10.1073/pnas.1922563117
27. El-Husseini AE, Schnell E, Chetkovich DM, Nicoll RA, Bredt DS (2000) PSD-95 involvement in maturation of excitatory synapses. Science 290 (5495):1364-1368
28. Nery FC, Armata IA, Farley JE, Cho JA, Yaqub U, Chen P, da Hora CC, Wang Q, Tagaya M, Klein C, Tannous B, Caldwell KA, Caldwell GA, Lencer WI, Ye Y, Breakefield XO (2011) TorsinA participates in endoplasmic reticulum-associated degradation. Nat Commun 2:393. doi:10.1038/ncomms1383
29. Chen P, Burdette AJ, Porter JC, Ricketts JC, Fox SA, Nery FC, Hewett JW, Berkowitz LA, Breakefield XO, Caldwell KA, Caldwell GA (2010) The early-onset torsion dystonia-associated protein, torsinA, is a homeostatic regulator of endoplasmic reticulum stress response. Hum Mol Genet 19 (18):3502-3515. doi:10.1093/hmg/ddq266
30. Cho JA, Zhang X, Miller GM, Lencer WI, Nery FC (2014) 4-Phenylbutyrate attenuates the ER stress response and cyclic AMP accumulation in DYT1 dystonia cell models. PLoS One 9 (11):e110086. doi:10.1371/journal.pone.0110086
31. Hewett J, Ziefer P, Bergeron D, Naismith T, Boston H, Slater D, Wilbur J, Schuback D, Kamm C, Smith N, Camp S, Ozelius LJ, Ramesh V, Hanson PI, Breakefield XO (2003) TorsinA in PC12 cells:

localization in the endoplasmic reticulum and response to stress. J Neurosci Res 72 (2):158-168. doi:10.1002/jnr.10567

32. Cnop M, Toivonen S, Igoillo-Esteve M, Salpea P (2017) Endoplasmic reticulum stress and eIF2alpha phosphorylation: The Achilles heel of pancreatic beta cells. Mol Metab 6 (9):1024-1039. doi:10.1016/j.molmet.2017.06.001
33. Oyadomari S, Mori M (2004) Roles of CHOP/GADD153 in endoplasmic reticulum stress. Cell Death Differ 11 (4):381-389. doi:10.1038/sj.cdd.4401373
34. Beauvais G, Rodriguez-Losada N, Ying L, Zakirova Z, Watson JL, Readhead B, Gadue P, French DL, Ehrlich ME, Gonzalez-Alegre P (2018) Exploring the Interaction Between eIF2alpha Dysregulation, Acute Endoplasmic Reticulum Stress and DYT1 Dystonia in the Mammalian Brain. Neuroscience 371:455-468. doi:10.1016/j.neuroscience.2017.12.033
35. Costa-Mattioli M, Sonenberg N, Richter JD (2009) Translational regulatory mechanisms in synaptic plasticity and memory storage. Prog Mol Biol Transl Sci 90:293-311. doi:10.1016/S1877-1173(09)90008-4
36. Di Prisco GV, Huang W, Buffington SA, Hsu CC, Bonnen PE, Placzek AN, Sidrauski C, Krnjevic K, Kaufman RJ, Walter P, Costa-Mattioli M (2014) Translational control of mGluR-dependent long-term depression and object-place learning by eIF2alpha. Nat Neurosci 17 (8):1073-1082. doi:10.1038/nn.3754
37. Godin JD, Creppe C, Laguesse S, Nguyen L (2016) Emerging Roles for the Unfolded Protein Response in the Developing Nervous System. Trends Neurosci 39 (6):394-404. doi:10.1016/j.tins.2016.04.002
38. Tajiri S, Oyadomari S, Yano S, Morioka M, Gotoh T, Hamada JI, Ushio Y, Mori M (2004) Ischemia-induced neuronal cell death is mediated by the endoplasmic reticulum stress pathway involving CHOP. Cell Death Differ 11 (4):403-415. doi:10.1038/sj.cdd.4401365
39. Nosyreva E, Kavalali ET (2010) Activity-dependent augmentation of spontaneous neurotransmission during endoplasmic reticulum stress. J Neurosci 30 (21):7358-7368. doi:10.1523/JNEUROSCI.5358-09.2010
40. Chen X, Winters C, Azzam R, Li X, Galbraith JA, Leapman RD, Reese TS (2008) Organization of the core structure of the postsynaptic density. Proc Natl Acad Sci U S A 105 (11):4453-4458. doi:10.1073/pnas.0800897105
41. Shin SM, Zhang N, Hansen J, Gerges NZ, Pak DT, Sheng M, Lee SH (2012) GKAP orchestrates activity-dependent postsynaptic protein remodeling and homeostatic scaling. Nat Neurosci 15 (12):1655-1666. doi:10.1038/nn.3259
42. Diering GH, Huganir RL (2018) The AMPA Receptor Code of Synaptic Plasticity. Neuron 100 (2):314-329. doi:10.1016/j.neuron.2018.10.018
43. Luscher C, Malenka RC (2012) NMDA receptor-dependent long-term potentiation and long-term depression (LTP/LTD). Cold Spring Harb Perspect Biol 4 (6). doi:10.1101/cshperspect.a005710
44. Gong LW, De Camilli P (2008) Regulation of postsynaptic AMPA responses by synaptojanin 1. Proc Natl Acad Sci U S A 105 (45):17561-17566. doi:10.1073/pnas.0809221105

45. Fischer M, Kaech S, Wagner U, Brinkhaus H, Matus A (2000) Glutamate receptors regulate actin-based plasticity in dendritic spines. Nat Neurosci 3 (9):887-894. doi:10.1038/78791
46. Bellone C, Nicoll RA (2007) Rapid bidirectional switching of synaptic NMDA receptors. Neuron 55 (5):779-785. doi:10.1016/j.neuron.2007.07.035
47. Gray JA, Shi Y, Usui H, During MJ, Sakimura K, Nicoll RA (2011) Distinct modes of AMPA receptor suppression at developing synapses by GluN2A and GluN2B: single-cell NMDA receptor subunit deletion in vivo. Neuron 71 (6):1085-1101. doi:10.1016/j.neuron.2011.08.007
48. Zhang Y, Cudmore RH, Lin DT, Linden DJ, Huganir RL (2015) Visualization of NMDA receptor-dependent AMPA receptor synaptic plasticity in vivo. Nat Neurosci 18 (3):402-407. doi:10.1038/nn.3936

Figures

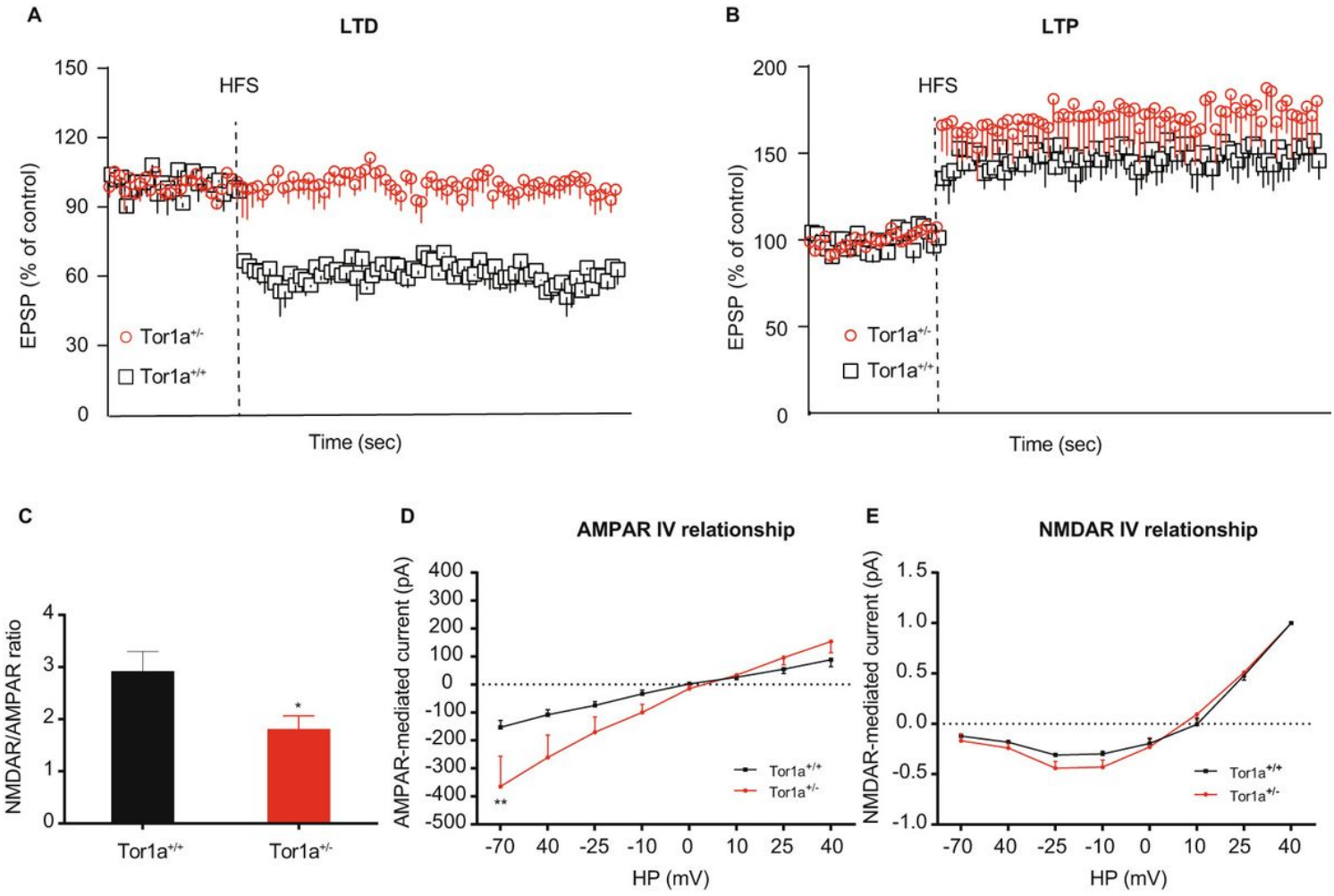

Figure 1

Altered striatal long-term synaptic plasticity in Tor1a+/- mice. (A) Time-course of corticostriatal LTD expression in SPNs from Tor1a+/+ and Tor1a+/- mice. HFS protocol induces LTD in SPNs recorded from Tor1a+/+ mice ($P<0.05$), but not from Tor1a+/- mice ($P>0.05$). (B) Time-course of corticostriatal LTP

expression in SPNs from Tor1a+/+ and Tor1a+/- mice. In Tor1a+/- SPNs LTP showed a tendency to increase compared with wild-type SPNs. (C) Summary plot of NMDA/AMPA current ratio calculated in SPNs from Tor1a+/+ and Tor1a+/- mice. A significant decrease of NMDA/AMPA ratio was detected in Tor1a+/- mice, compared to Tor1a+/+ mice. (D) AMPAR-mediated currents recorded at different HP in Tor1a+/+ and Tor1a+/- SPNs. The I-V relationship shows a significant increase in the current recorded at more hyperpolarized range from Tor1a+/- SPNs (HP= -70 mV, P<0.01). (E) Normalized IV relationships of NMDAR-mediated currents show no difference between genotypes (P >0.05).

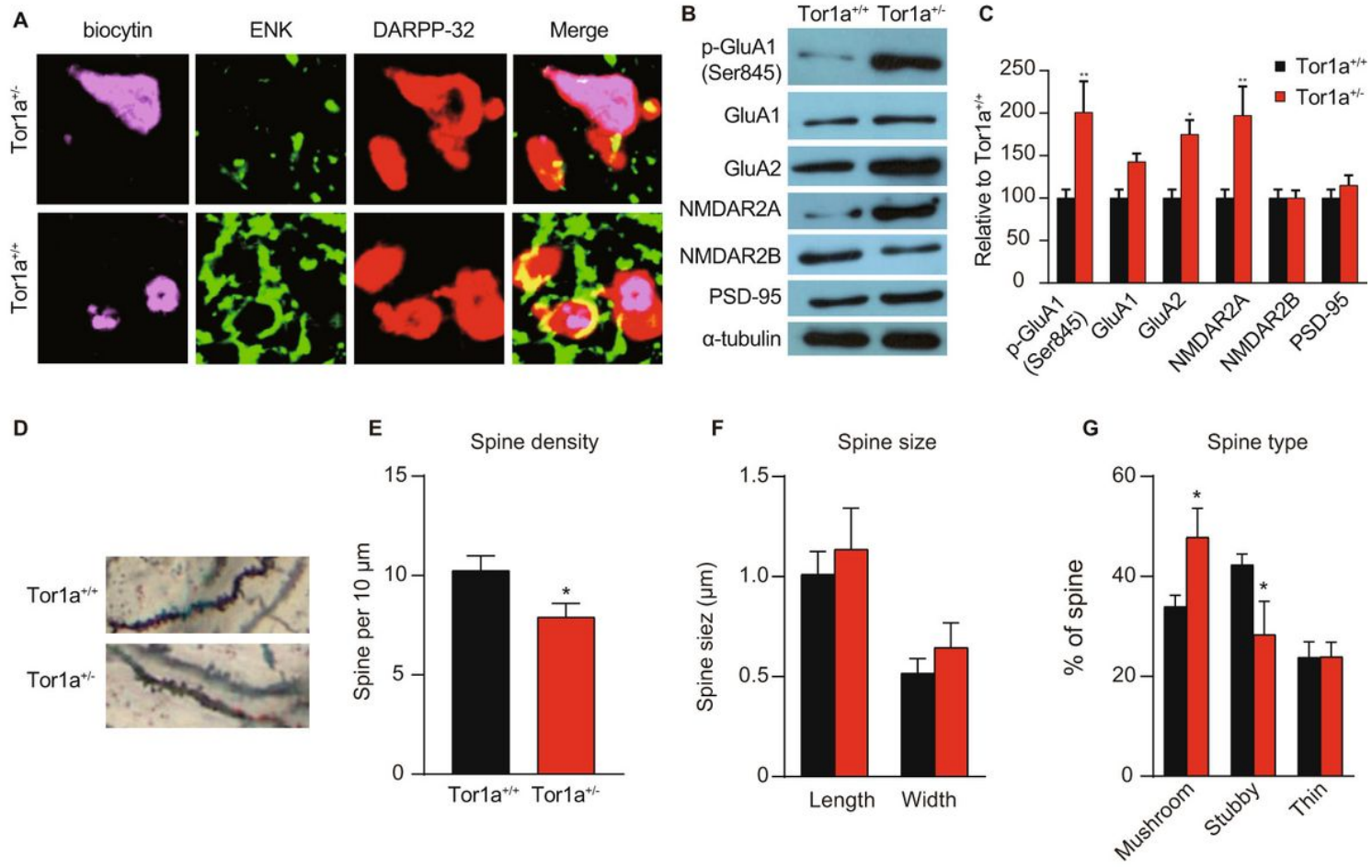

Figure 2

Altered molecular markers and morphology of synapse in Tor1a+/- mice. (A) Representative confocal images from two SPNs recorded in Tor1a+/- and Tor1a+/+ slices (scale bar: 10 µm). Recording electrodes were filled with biocytin (pink) and SPNs were immunolabelled with anti-ENK (green) and anti-DARPP-32 (red). ENK-negative SPNs from Tor1a+/- failed to induce LTD. (B) WB analysis for p-GluA1 (Ser845), GluA1, GluA2, NMDAR2A, NMDAR2B, PSD-95 and alpha-tubulin in Tor1a+/- and age-matched Tor1a+/+ mice. (C) Histogram shows the quantification of protein levels following normalization on alpha-tubulin in Tor1a+/- and age-matched Tor1a+/+ mice. All values are mean ± SEM expressed as % of Tor1a+/+ mice. (D) Representative images show spine morphology of Tor1a+/- and age-matched Tor1a+/+ mice. (E) Histogram representing dendritic spine density in Tor1a+/- and Tor1a+/+ SPNs. Tor1a+/- SPNs exhibited an overall decrease of dendritic spine density (P<0.05). (F, G) Histograms showing the

quantification of dendritic spine size (F, spine length and head width) and dendritic spine type (G, mushroom, stubby, thin) in Tor1a+/- and age-matched Tor1a+/+ mice. A larger number of mushroom-type spines and a concomitant smaller number of stubby-type spines were found (both P<0.05)

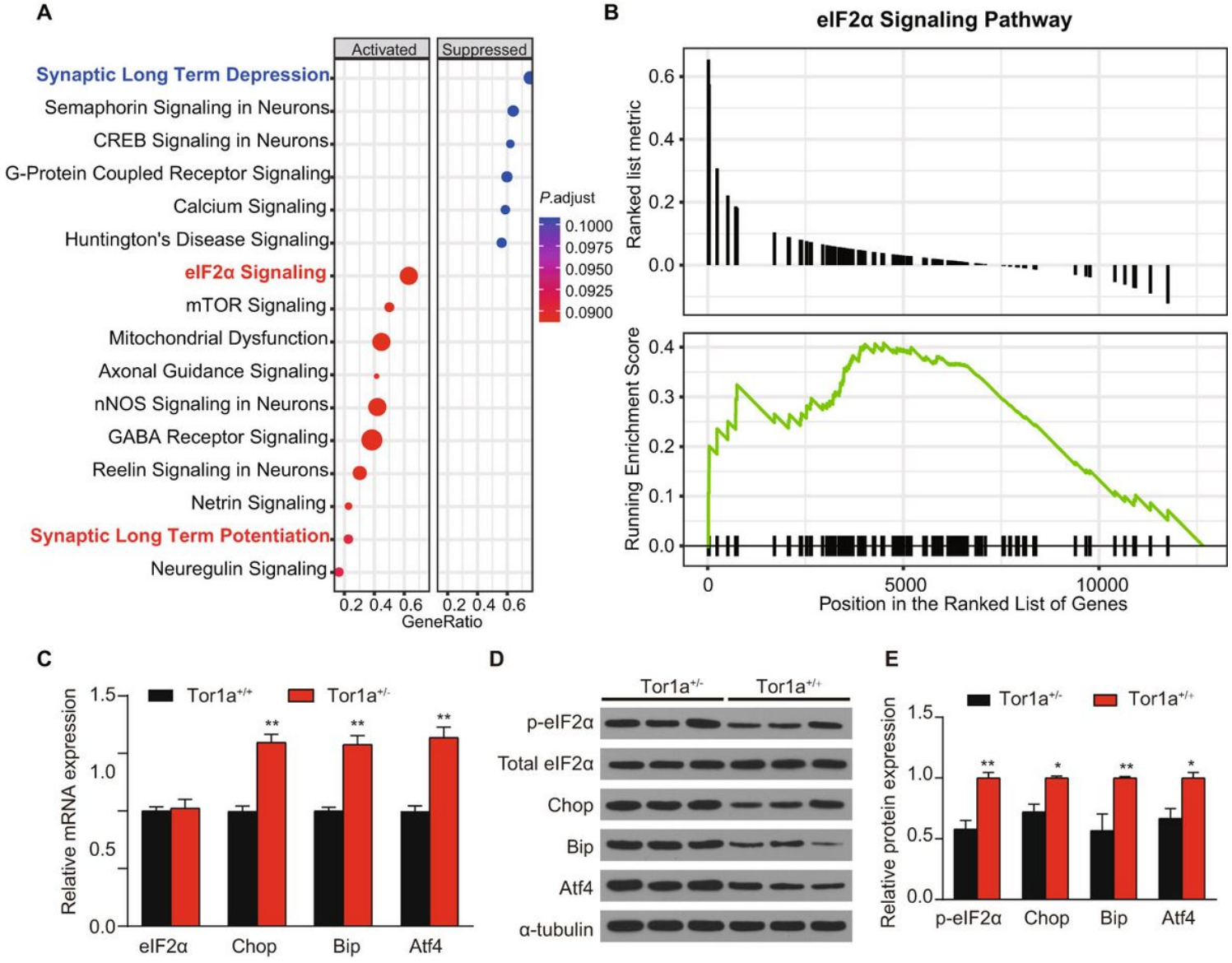

Figure 3

Abnormal eIF2α signaling and ER stress in Tor1a+/- mice. (A) Ingenuity pathway analysis (IPA) was completed to identify significantly dysregulated canonical pathways. The top 15 pathways generated with the DEGs. (B) Gene Set Enrichment Analysis (GSEA) was applied to further confirm the up-regulated eIF2α signaling in Tor1a+/- mice. (C) Levels of mRNA in striatal lysates were measured by RT-qPCR. (D&E) Representative western blots of striatal lysates (D). Quantification of protein expression in striatum ais shown (n: 3 per group). Data are represented as mean ±SEM.

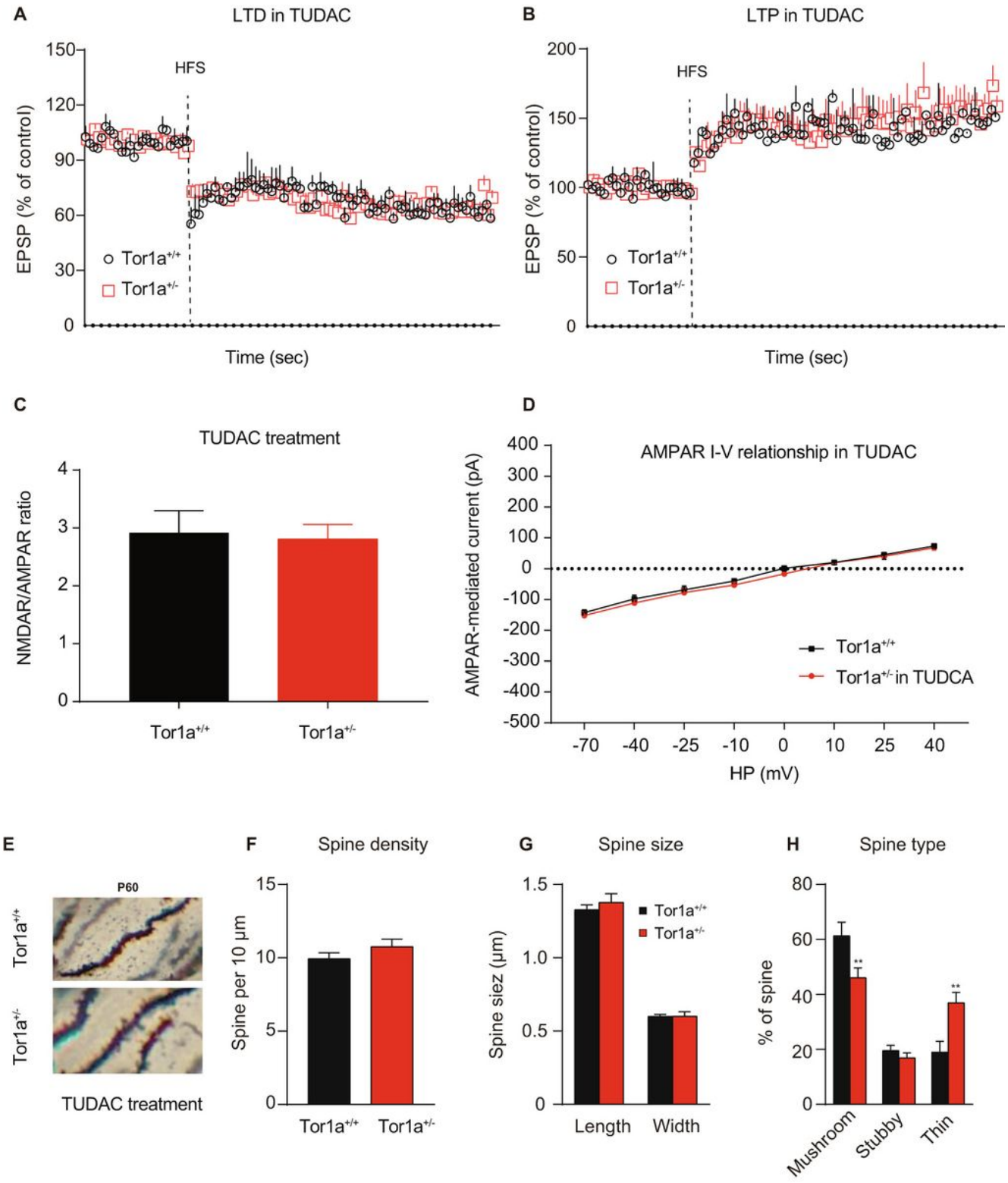

Figure 4

ER stress inhibitor rescues long-term memory deficit in Tor1a+/- mice. (A) Time-course of corticostriatal LTD expression in SPNs from Tor1a+/+ and Tor1a+/- mice. After in vivo treatment with TUDAC, the HFS protocol induced corticostriatal LTD expression in Tor1a+/- mice. (B) Time-course of corticostriatal LTP expression in SPNs from Tor1a+/+ and Tor1a+/- mice. LTP amplitude in Tor1a+/- mice was comparable to that of SPNs from Tor1a+/+ littermates. (C) Summary plot of NMDA/AMPA current ratio calculated in

SPNs from Tor1a+/+ and Tor1a+/- mice. treatment with TUDAC completely normalized the NMDAR/AMPAR ratio in Tor1a+/- mice (P>0.05). (D) AMPAR-mediated currents recorded at different HP in Tor1a+/+ and Tor1a+/- SPNs. The IV curve of AMPAR-EPSC also revealed no significant difference between genotypes (P>0.05). (E) Representative images show dendrites of Tor1a+/- and Tor1a+/+ SPNs. (F-H) Histogram representing the quantification of dendritic spine density (F), dendritic spine size (G, spine length and head width) and dendritic spine type (H, mushroom, stubby, thin) in Tor1a+/- and Tor1a+/+ SPNs.

Supplementary Files

This is a list of supplementary files associated with this preprint. Click to download.

- SupplementaryMaterialsV1.02021.01.23.docx
- FigureS1.eps
- FigureS2.eps
- FigureS3.eps